



INCORPORATION OF LARGER Gd^{3+} RARE EARTH IONS INTO Mn-Cr-Fe NANOCRYSTALLINE POWDER ALLOYS

KIRTI DESAI¹, SUPRIYA KADAM², RAM KADAM³, SAGAR E. SHIRSATH⁴

¹ Pacific University, Udaipur, Rajasthan.

² S. M. P. College, Murum, Tq. Omerga, Dsit. Osmanabad (M.S.)

³ Materials Science research lab, Shrikrishna Mahavidyalaya Gunjoti, Osmanabad, MS, India

⁴ Spin Device Technology Center, Department of Information Engineering, Shinshu University, Nagano, Japan

Abstract:

Sol-gel auto combustion method is used to synthesize the rare earth Gd^{3+} incorporated Mn-Cr-Fe nanocrystalline powder. The synthesized powder samples were annealed at 600 °C for 4 h. X-ray diffraction data were used to evaluate the structure of the prepared samples. X-ray diffraction pattern shows the presence of Gd^{3+} ions. Rare earth Gd^{3+} ions form the secondary phase as evidenced by the X-ray diffraction pattern. Lattice constant (a), X-ray density (d_x), Crystallite size (D_{XRD}), hopping lengths (L_A and L_B), allied parameters such as tetrahedral and octahedral bond length (d_{Ax} and d_{Bx}), tetrahedral edge, shared and unshared octahedral edge (d_{AXE} , d_{BXE} and d_{BXEU}) were calculated using X-ray diffraction data. Hopping lengths and allied parameters varied with Gd^{3+} incorporation.

KEYWORDS:

Rare earth ion; Sol-gel method, hopping length

INTRODUCTION:

Magnetic nanoparticles are gaining importance due to their potential applications in high-density magnetic recording, magnetic fluid, biomedical and microwave applications etc. During the last few decades, ferrites have been studied extensively because of their importance in basic as well as in applied research [1,2].

Spinels with rare earth (RE) ions have attracted great attention in the material science field because of their interesting properties, such as infrared emission, catalytic, photoelectric, and magnetic properties [3,4]. It is known that the magnetic behaviour of the ferrimagnetic oxide compounds is largely governed by the Fe-Fe interaction (the coupling of the spins of the 3d electrons). By introducing R ions in the spinel lattice, the R-Fe interactions appear too (3d-4f coupling), which can lead to small changes in the magnetization and Curie temperature [5-7].

Many research groups have investigated to enhance the magnetic property of magnetic materials such as manganese ferrite. $MnFe_2O_4$ is a ferrimagnet ($T_N = 560$ K) having the spinel structure with two inequivalent sublattices of tetrahedral (A) and octahedral [B] symmetries for the magnetic ions sites [8-11]. It is found that small substitution of Fe^{3+} ions by Gd^{3+} ions may favorably influence the electromagnetic

properties of ferrites facilitating good magnetic characteristics for high frequency applications [12-15]. In this research we have made an attempt to study the effect of Gd³⁺ substitution on the structural properties of MnCrGd_xFe_{1-x}O₄ (x = 0.0, 0.05, 0.1 and 0.15)

EXPERIMENTAL

The ferrite powders were synthesized through sol-gel auto-combustion route to achieve homogeneous mixing of the chemical constituents on the atomic scale and better sinterability. AR grade manganese nitrate (Mn(NO₃)₂·6H₂O), chromium nitrate (Cr(NO₃)₃·9H₂O), gadolinium nitrate Gd(NO₃)₃·9H₂O, iron nitrate (Fe(NO₃)₃·9H₂O) and citric acid (C₆H₈O₇·H₂O), were used to prepare the MnCrGd_xFe_{1-x}O₄ (x = 0.0, 0.05, 0.1 and 0.15) ferrite compositions. Reaction procedure was carried out in air atmosphere without protection of inert gases. The molar ratio of metal nitrates to citric acid was taken as 1:3. The metal nitrates were dissolved together in a minimum amount of double distilled water to get a clear solution. An aqueous solution of citric acid was mixed with metal nitrates solution, then ammonia solution was slowly added to adjust the pH at 7. Then the solution was heated at 90 °C to transform into gel. When ignited at any point of the gel, the dried gel burnt in a self-propagating combustion manner until all gels were completely burnt out to form a fluffy loose powder. The auto-ignition of gel was carried out in glass beaker upon a hot plate. The auto-combustion was completed within a minute, yielding the brown-colored ashes termed as a precursor. The as prepared powder then annealed at 600 °C for 4 h.

Structural analysis of the powders were carried out on a Phillips X-ray diffractometer (Model 3710) using Cu-K radiation (=1.5405 Å).

RESULTS AND DISCUSSION

The XRD patterns of typical composition MnCrGd_{0.1}Fe_{0.9}O₄ (x = 0.1) ferrite nanocrystals synthesized at room temperature is shown in Fig. 1. The XRD lines are appeared to be broad. Further, the increase in intensity of X-ray diffraction with Gd³⁺ doping shows improved crystallinity of the materials. The X-ray analysis indicated the presence of GdFeO₃ ortho phase in the resulting compound due to reactivity of Gd³⁺ and Fe³⁺ [16]. The presence of the second phase (GdFeO₃) is due to the higher activity of Fe³⁺ ions with Gd³⁺ ions on the grain boundaries.

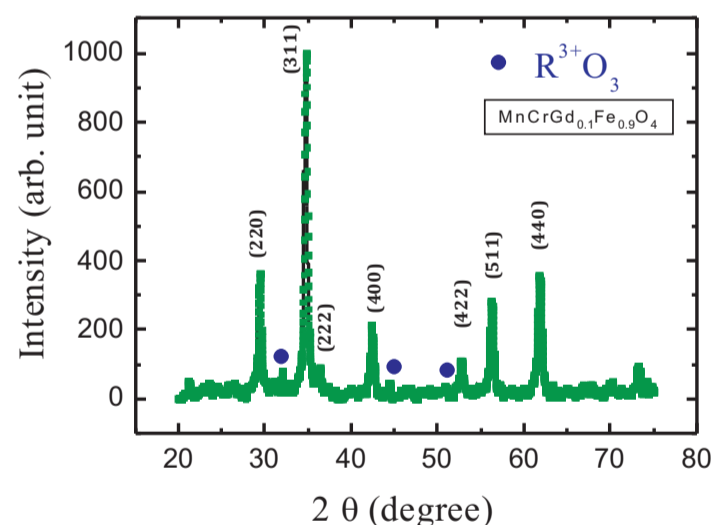


Fig. 1: X-ray diffraction pattern of the typical sample

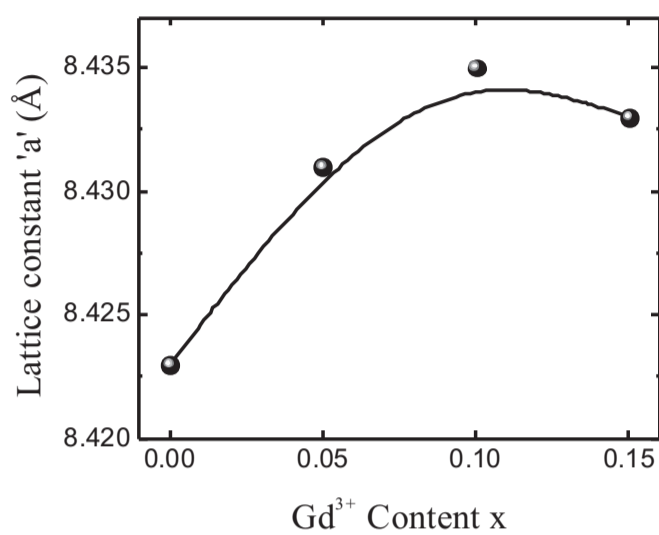


Fig. 2: Variation of lattice constant with Gd³⁺ content x

The lattice constants (a) are determined by using Bragg's law as a function of Gd³⁺ content [17]:

$$a = d\sqrt{(h^2 + k^2 + l^2)} \quad \mathbf{1}$$

where d is the inter-planer spacing and (hkl) is the index of the XRD reflection peak. The dependence of the lattice parameter on the Gd³⁺ content x is shown in Table 1 and Fig. 2 and shows non-linear behavior.

The X-ray density (d_x) of all the samples of the series was obtained by the following relation:

$$d_x = \frac{8M}{Na^3}$$

where 8 is the number of molecules per unit cell, 'M' is the molecular weight of sample, 'N' is the Avogadro's number and 'a' is lattice constant.

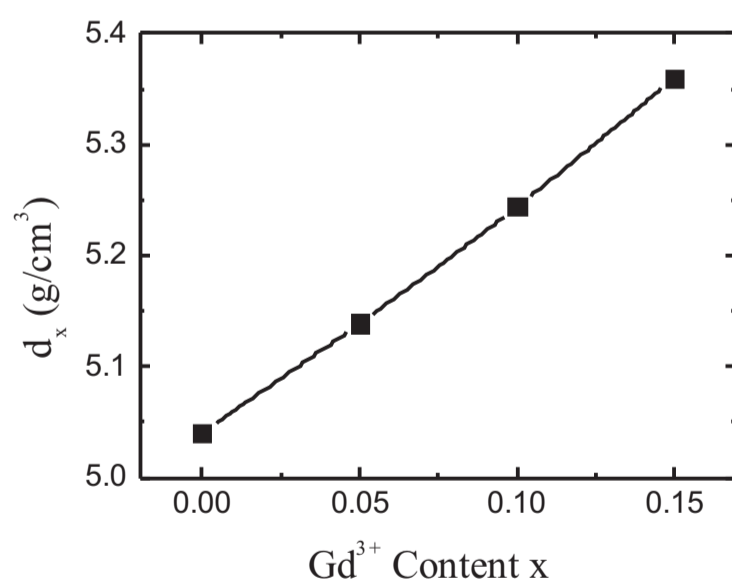


Fig. 3: Variation of X-ray density (dx) with Gd³⁺ content x

It is seen from Fig. 3 and Table 1 that the X-ray density increases linearly with the Gd³⁺ content x. Both the molecular weight and the volume of the unit cell for the doped ferrite increase with the Gd³⁺ content x, because of the replacement of larger Gd³⁺ for Fe³⁺, and the molecular weight has more increment when compared to the volume of the unit cell, therefore, the X-ray density increases with the Gd³⁺ content x.

Table 1

Lattice constant (a), X-ray density (d_x) and crystallite size (D_{XRD}) of MnCrGd_xFe_{1-x}O₄

Comp. x	a (Å)	d _x (g/cm ³)	D _{XRD} (nm)
0.00	8.423	5.041	12
0.05	8.431	5.139	15
0.10	8.435	5.244	20
0.15	8.433	5.360	17

The average crystallite diameter 'D_{XRD}' of powder estimated from the most intense (311) peak of XRD and using the Scherrer formula [17]:

$$D_{XRD} = \frac{0.9\lambda}{B \cos\theta}$$

where λ is the wavelength used in XRD, B is the full width of half maximum in (2), is the corresponding Bragg angle.

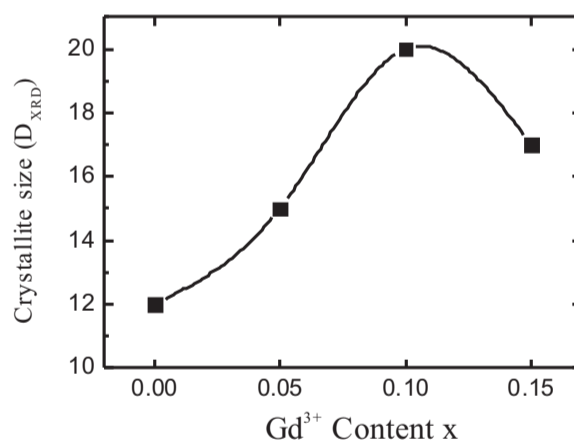


Fig. 4: Variation of crystallite size (D_{XRD}) with Gd³⁺ content x

Figure 4 and Table 1 shows that the crystallite diameter varies in the range of 12 to 20 nm with increase in Gd³⁺ substitution.

The allied parameters such as tetrahedral and octahedral bond length (d_{Ax} and d_{Bx}), tetrahedral edge, shared and unshared octahedral edge (d_{AXE}, d_{BXE} and d_{BXEU}) were calculated:

$d_{AX} = a \sqrt{3} (u-1/4)$	4
$d_{BX} = a [3u^2 - (11/4)u + 43/64]^{1/2}$	5
$d_{AXE} = a \sqrt{2} (2u-1/2)$	6
$d_{BXE} = a \sqrt{2}(1-2u)$	7
$d_{BXEu} = a [4u^2 - 3u + (11/16)]^{1/2}$	8

Figure 5 and Table 2 show that all the allied parameter increased for x 0.1 with the increase in Gd³⁺ substitution.

Table 2

Tetrahedral bond (d_{AX}), octahedral bond (d_{BX}), tetra edge (d_{AXE}) and octahedral edge (d_{BXE}) (shared and unshared) of MnCrGd_xFe_{1-x}O₄

Comp. 'x'	d_{AX} (Å)	d_{BX} (Å)	Tetra edge (Å)		
			d_{AXE}	Shared	unshared
0.00	1.911	2.059	3.120	2.835	2.986
0.05	1.913	2.061	3.123	2.837	2.988
0.10	1.914	2.062	3.125	2.839	2.990
0.15	1.913	2.061	3.124	2.838	2.989

The variation of allied parameters is related to the variation in lattice constant. In the present study smaller Fe³⁺ ions are replaced by the larger Gd³⁺ ion, this difference in the ionic radii is reflected in the lattice constant and also in the variation of all the allied parameters.

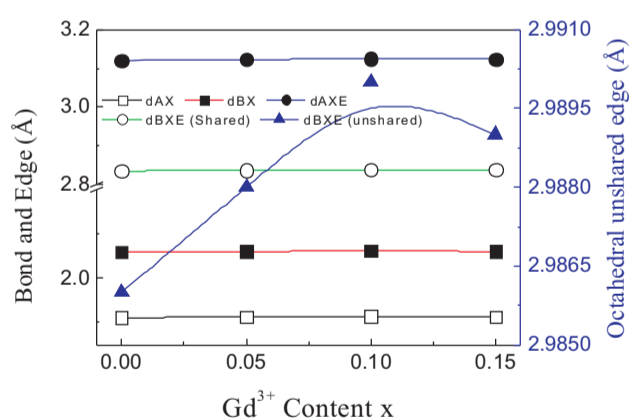


Fig. 5: Variation of Tetrahedral bond (d_{AX}), octahedral bond (d_{BX}), tetra edge (d_{AXE}) and octahedral edge (d_{BXE}) (shared and unshared) with Gd³⁺ content.

The hopping length for A-site (L_A) and B-sites (L_B) are calculated using the values of lattice constant.

$$L_A = a\sqrt{\frac{3}{4}} \tag{9}$$

$$L_B = a\sqrt{\frac{2}{4}} \tag{10}$$

Table 3 and Fig. 6 shows the variation of hopping lengths (L_A and L_B) with different concentration of Gd³⁺ ions substitution. The hopping length distance at both the available sites between the constituent ions in composition in increased with the Gd₃₊ substitution.

Table 3
Hopping length L_A and L_B of MnCrGd_xFe_{1-x}O₄

Comp. x	Hopping length	
	L _A (Å)	L _B (Å)
0.00	3.6473	2.9780
0.05	3.6507	2.9808
0.10	3.6525	2.9822
0.15	3.6516	2.9815

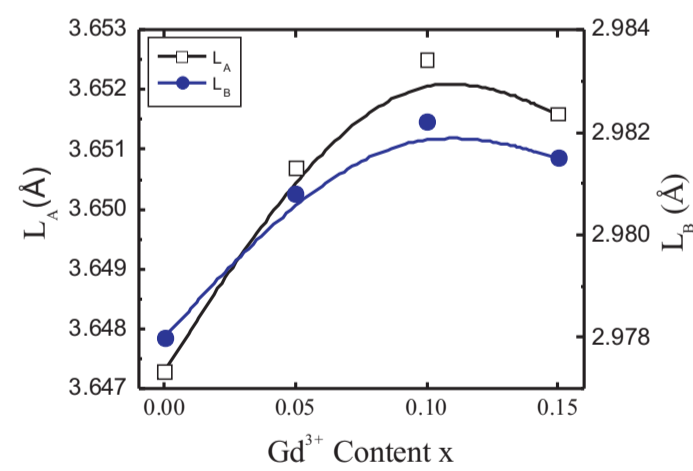


Fig. 6: Variation of hopping lengths (L_A and L_B) with Gd³⁺ substitution.

CONCLUSIONS

Rare earth Gd³⁺ substituted Mn-Cr ferrites nanoparticles with a chemical formula MnCrGd_xFe_{1-x}O₄ were successfully synthesized by the sol-gel auto combustion method. Variation of lattice constant is related to the difference in the ionic radii of Gd³⁺ and Fe³⁺ ions. X-ray density found to increase with the increase in Gd³⁺ ions, this increase in d_x is related to the molecular weight of Gd³⁺ ions. The average crystallite size initially increased followed by decreasing trend with Gd³⁺ substitution. Ion jump length of tetrahedral A- and octahedral B-sites and all the allied parameters shows dependence of Gd³⁺ substitution. Behaviour of ion jump lengths and allied parameters are related to the larger ionic radii of La³⁺ ions as compared to that of Fe³⁺ ions.

REFERENCES

- [1] Sagar E Shirsath, "Synthesis condition reflected structural and magnetic properties of Li^{0.5}Cr_{0.5}Fe₂O₄ nanoparticles" in 'Magnetic Nanoparticles: Properties, Synthesis and Applications' edited by Beate Acklin and Edon Lautens, Nova publishers, New York, 2012.
- [2] Sagar E. Shirsath, R.H. Kadam, Anil S. Gaikwad, Ali Ghasemi, Akimitsu Morisako, J. Magn. Magn. Mater. 323 (2011) 3104.
- [3] Ying Zhang, Dijiang Wen, Mater. Sci. Engg. B 172 (2010) 331–335.
- [4] Sagar E. Shirsath, R. H. Kadam, S. M. Patange, M. L. Mane, Ali Ghasemi, Akimitsu Morisako, Appl. Phys. Lett. 100 (2012) 042407.
- [5] N. Rezlescu and E. Rezlescu, Solid State Commun. 88 (1993) 139-141.
- [6] Sagar E. Shirsath, Santosh S. Jadhav, B. G. Toksha, S. M. Patange, and K. M. Jadhav, Scri. Mater. 64 (2011) 773–776
- [7] Sagar E. Shirsath, S. S. Jadhav, B. G. Toksha, S. M. Patange and K. M. Jadhav, J. Appl. Phys. 110 (2011) 013914-1-8.
- [8] R. H. Kadam, A. R. Biradar, M. L. Mane and Sagar E. Shirsath, J. Appl. Phys. 112 (2012) 043902
- [9] Q. Song, Y. Ding, Z. L. Wang and Z. J. Zhang, Chem. Mater. 19 (2007) 4633-4638
- [10] Q. Song and Z. J. Zhang, J. Am. Chem. Soc. 134 (2012) 10182- 10190
- [11] S. Matzen et al. Phys. Rev. B 83 (2011) 184402
- [12] N. Rezlescu, E. Rezlescu, D.P. Popa, L. Rezlescu, J. Alloys Compd., 275-277 (1998) 657
- [13] Jagdish Chand, M. Singh, J. Alloys Compd. 486 (2009) 376–379
- [14] J.C. Apesteguy, P.G. Bercoff, S.E. Jacobo, Physica B 398 (2007) 200–203
- [15] Anu Rana, O.P. Thakur, Vinod Kumar, Mater. Lett. 65 (2011) 3191–3192
- [16] A. B. Gadkari, Tukaram J. Shinde, Pramod N. Vasambekar, J. Magn. Magn. Mater. 322 (2010) 3823–3827.
- [17] B. D. Cullity, Elements of X-ray diffraction, Addison-Wesley, London, 1959